Making 3D Replicas Using a Flatbed Scanner and a 3D Printer

Vaclav Skala[1], Rongjiang Pan[2], and Ondrej Nedved[1]

[1] Faculty of Applied Sciences, University of West Bohemia
CZ 30614 Plzen, Czech Republic
[2] School of Computer Science and Technology, Shandong University
250101 Jinan, China

Abstract. This paper describes a novel approach to making 3D replicas of nearly flat objects using a flatbed scanner and a 3D printer. The surface reconstruction is based on the fact that the light in a flatbed scanner shines under a given constant angle and the CCD sensor records different intensities depending on the angle between a local normal vector of a micro-facet and the vector towards the light source position. The scanned object is rotated by 90° and thus four different images are obtained. It enables normal vector estimation followed by a surface reconstruction based on analogy with solution of partial differential equations. 3D replicas are produced using a 3D printer based on the data from the surface reconstruction. Due to high resolution of the flatbed scanner, resulting replicas are of a high precision as well. This method can be used e.g. in making replicas of archaeological parts.

Keywords: computer graphics, 3D surface reconstruction, 3D printing, digital archaeology.

1 Introduction

Surface reconstruction methods are used in many applications. They are based on laser scanning or other similar techniques, like deflectometry. Most of the devices have difficulties in scanning small objects or objects with fine details.

This paper presents a new approach for a surface reconstruction and 3D print of nearly flat small objects using a flatbed scanner. The approach is based on normal vectors map computation from the scanned image followed by a surface reconstruction and thereafter construction of a final 3D object representing the reconstructed surface. The size of the object is limited by the scanning area – usually A4 or "letter" format. Due to high hardware resolution of a scanner, usually up to 4800 dpi, scanning precision is high and it enables to reconstruct a surface with very fine details. It is expected that the given approach can be used especially in producing 3D replicas of nearly flat objects, like coins or rough fabrics etc.

B. Murgante et al. (Eds.): ICCSA 2014, Part VI, LNCS 8584, pp. 76–86, 2014.

2 Related Work

As for the related work, there are several papers to be mentioned. M.K.Johnson et al. [5] from MIT extended his former work cooperating with Adelson [4] and proposed a texture independent method for getting a surface with a fine resolution. On the other hand a sophisticated device for using the mentioned method is required. The former work of Johnson and Adelson [4] itself uses a special elastomer, which is „pushed into a relief", to get a texture independent surface, which is then reconstructed using a well-known photometric stereo algorithm. Chen, Goesele and Seidel [2] proposed a method for intermediate surface detail reconstruction from specularity. As for the prior partially related work, Liu et al. [6] introduced algorithms for synthesis of bidirectional texture functions (BTF) for gaining the texture information and thus material dependence. Our approach does not require any specially constructed hardware, can be used for reconstruction of either fine cloths or fabrics, as in the mentioned papers, and well as for glossy objects like polished coins too.

3 Scanning

In photometric stereo, at least three images of the surface are required [12]. Typically, more than the minimum three images are used in practice when considering the noise. Digital cameras can be used to take multiple images from the same view point illuminated with different light sources of known position. Multiple images of an object at different orientations can also be scanned with a flatbed scanner. To make the process easier and robust, we take scans rotated by 90 degrees. In order to make the orientation of the object as accurate as possible along the side of the scanner platen, we utilize a square clamp to fix the scanned object. A planar checkerboard pattern is glued on the surface of the clamp and utilized in the multiple scans registration. The checkerboard corners are automatically extracted in subpixel precision. We find an optimal rigid transformation using the corresponding corners in each scan. After aligning the other three scans to the first scan, we cut out the image regions that are out of interest. Fig.1 shows four registered images of an 'Yi Jiao' coin at different orientations along the flatbed scanner.

(a) 0 degree (b) 90 degree (c) 180 degree (d) 270 degree

Fig. 1. Four scans of an 'Yi Jiao' coin

4 Normal Vectors Reconstruction

The light source of a flatbed scanner is linear and placed at a fixed angle α with respect to the scanner platen. According to [9], the angle α is approximately $\pi / 6$. Each point on the scanned surface has a normal n and albedo ρ. For the scan taken at zero degree orientation, we define a left-handed coordinate system as shown in Fig.2, whose origin is at the surface point considered. The x-axis is parallel to the CCD sensor array at the surface point considered, xy-plane is the scanner platen and z-axis points straight down. The light source is approximated by a line segment extending from $-l$ to $+l$ in the x-axis direction and is offset by a in the y-direction and b in the z-direction. We define $n = [n_x, n_y, n_z]^T$ as a normalized surface normal at the point and $l = (x, a, b)^T / \sqrt{x^2 + a^2 + b^2}$ the normalized lighting direction vector along the linear light source.

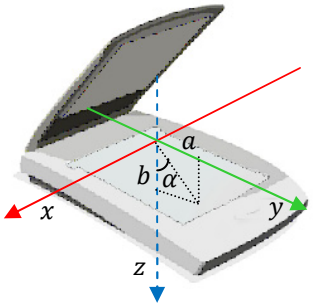

Fig. 2. Coordinate system at orientation zero degree

The observed intensity of such a surface point is then:

$$I_0 = \varrho \int_{-l}^{l} \langle \boldsymbol{n}, \boldsymbol{l} \rangle dx = \varrho \int_{-l}^{l} \frac{n_x x + n_y a + n_z b}{\sqrt{x^2 + a^2 + b^2}} dx = \varrho(n_y a + n_z b) \int_{-l}^{l} \frac{1}{\sqrt{x^2 + a^2 + b^2}} dx = \varrho s(n_y a + n_z b) \tag{1}$$

where:

$$s = \int_{-l}^{l} \frac{1}{\sqrt{x^2 + a^2 + b^2}} dx = 2 l n \frac{l + \sqrt{l^2 + a^2 + b^2}}{\sqrt{a^2 + b^2}} \tag{2}$$

as:

$$\int_{-l}^{l} \frac{n_x x}{\sqrt{x^2 + a^2 + b^2}} dx = 0 \tag{3}$$

is an odd (anti-symmetrical) function on the interval $\langle -l, l \rangle$.

In the same way, scanning the same surface point with the object rotated by $90, 180$ and 270 degrees, we get:

$$I_{90} = \varrho s(-n_x a + n_z b) \tag{4}$$

$$I_{180} = \varrho s\big(-n_y a + n_z b\big)$$

$$I_{270} = \varrho s(n_x a + n_z b)$$

We arrange the four equations (1) and (4) into a matrix equation which can be solved using linear least-squares. Its solution is:

$$\varrho s b n_x = (I_{270} - I_{90})/(2\ tan\alpha) \tag{5}$$

$$\varrho s b n_x = (I_0 - I_{180})/(2\ tan\alpha)$$

$$\varrho s b n_y = (I_0 + I_{90} + I_{180} + I_{270})/4$$

where: $\tan\alpha = a\ /\ b$. Finally, the normal n at this point of the surface is obtained and normalized.

Fig.3 shows the computed normal maps of the Yi Jiao coin, a game coin and a piece of a fine fabric. To visualize the normal map, n_x, n_y and n_z values of the surfaces' normals are mapped to RGB components respectively, i.e., n_x maps from $(-1.0,1.0)$ to red $(0,255)$, n_y maps from $(-1.0,1.0)$ to green $(0,255)$ and n_z maps from $(0.0,1.0)$ to blue $(0,255)$.

Fig. 3. Normal map of two coins and a piece of a fine fabric

When the normal map is computed, there is a question of how to reconstruct a surface of the object.

5 Surface Reconstruction

Surface reconstruction is usually based on points given by scanning etc. However, we have a slightly different task as we have a map of normal vectors and a boundary of the given object. This is a classical formulation of the boundary problem known from the partial differential equations, namely from computational physics field, e.g. heat diffusion computation etc.

It can be seen that for each row or column we have values at the boundary of the object and inside of such an interval we have only normal vectors, e.g. derivatives.

Derivatives can be estimated using centered difference as:

$$\frac{\partial f}{\partial x} \approx \frac{f(x+h,y) - f(x-h,y)}{2h} \tag{6}$$
$$\frac{\partial f}{\partial y} \approx \frac{f(x,y+h) - f(x,y-h)}{2h}$$

where h is an increment in the x and y axis and in our case it is set as $h = 1$.

When using a direct solution, we can reformulate the problem as:

$$2f_x = f(x+1,y) - f(x-1,y) \tag{7}$$

$$2f_y = f(x,y+1) - f(x,y-1) \tag{8}$$

Let us consider a normal map of a size $M \times N$. Avoiding normals at the border leaves us $(M-2) \times (N-2)$ inner points to compute the surface for. There are two equations for each inner point, adding the boundary conditions gives us an overdetermined system of linear equations with approximately $2 \cdot (M \cdot N)$ equations for $M \cdot N$ points to be computed.

Even though the size of the linear system is very large, it can be solved efficiently considering that the matrix is sparse. It can be seen that for this linear system of equations to be solved, least square error estimation must be applied, while minimizing:

$$\min \sum |s_x - s_y|^2 \tag{9}$$

Where s_x is height of the surface according to the first condition from (7) and s_y height of the surface according to the second condition from (8).

6 3D Print

Surface generation itself is quite simple as the surface reconstruction produces a $2\,{}^1\!/_2\,D$ height field on a rectangular grid. Therefore tessellation to a triangular mesh is straightforward.

For 3D print a closed volume is actually needed. It means that additional surfaces have to be added, i.e. a surface representing a border of the given object of a specified height and also bottom surface of the object. It should be noted that such final surface has to be print-ready, i.e. consistent orientation of facets, with no holes etc.

Now the scanned object is represented as a triangulated surface having its volume and can be printed out on a 3D printer.

7 Experimental Results

Normal vectors reconstruction from scanned objects on a flatbed scanner was verified on several types of objects. For a surface reconstruction a simple approach based on an analogy with partial differential equations (PDE) with boundary condition formulation was used.

Our approach to surface reconstruction using a flatbed scanner was verified on different coins. Fig.4, 5 and 6 show our results, from left to right the original scan, a normal map, a reconstructed $2\frac{1}{2}D$ surface and a resulting up-scaled copy printed on a 3D printer.

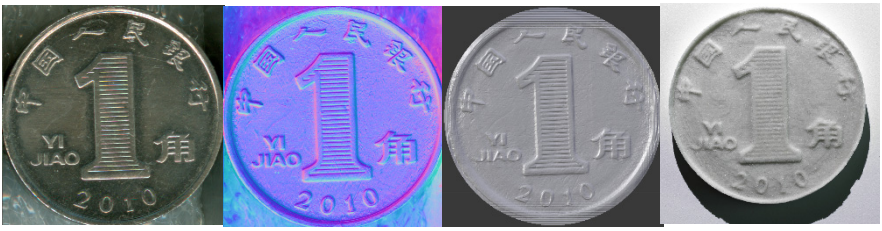

Fig. 4. Results of a 'Yi Jiao' coin. Left to right: original, normals, reconstruction, 3D print.

Fig. 5. Results of a '2 Kč' coin. Left to right: original, normals, reconstruction, 3D print

Fig. 6. Results of a '20 Kč' coin. Left to right: original, normals, reconstruction, 3D print

It should be noted that we set $h = 1$ in the difference estimation for simplicity of computation. The actual height of the reconstructed surface is to be adjusted manually.

Table 1. Experimental data for a coin reconstruction with 1683×1557 points

	Normal map computation	Surface reconstruction
64 bits	68 [ms]	18 959 [ms]
32 bits	110 [ms]	24 289 [ms]

For experiments a standard PC was used – 3.16 GHz 12 GB RAM 64 bits, Windows 8 Professional x64 and a standard scanner with only 600 dpi was used. As for the computation times, as shown in Table 1, the normal map acquisition is of an algorithmic complexity $O(N)$, where N is the number of elements of an image, and therefore very fast in contrast with the surface computation, where a linear equations system of $N{\sim}2\,mil.$ is solved. A 32 bit version of the software is available too.

For 3D print the ZPrinter 650 powder based 3D printer was used with 0.1 mm particle size.

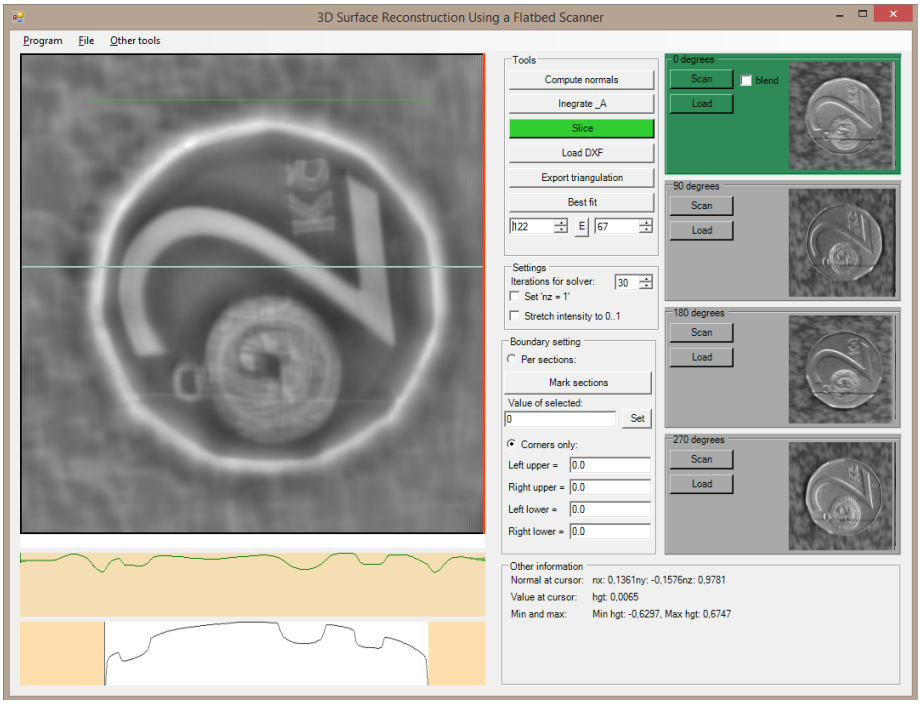

Fig. 7. The implemented user interface

Fig.7 presents user interface of the developed application. After loading 4 scanned images, each rotated by 90°, the normal map is computed followed by surface reconstruction and data export for 3D print. A comparison of a slice with an exact measurement is available too.

8 Comparison of the Reconstruction with Original

Additional experiments were made to compare the reconstructed surface to the real surface. Exact slices of coins used for this experiment were measured with a precision of 5 micrometers, which is sufficient for the used scanner having 600 dpi resolution.

Fig.8 to Fig.11 show a comparison of slices of the original coins and slices of their corresponding reconstructed models. An average error for all four coins can be found in Table 2.

Table 2. Average absolute error of the reconstruction compared to the original coin

	2 Kč	20 Kč	5 Kč	10 Kč
Average error	0.0342 mm	0.0399 mm	0.0409 mm	0.0270 mm

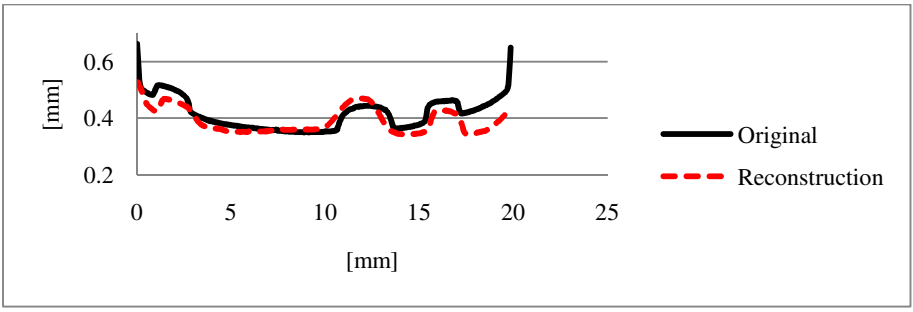

Fig. 8. Comparison of reconstruction of a '2 Kč' coin

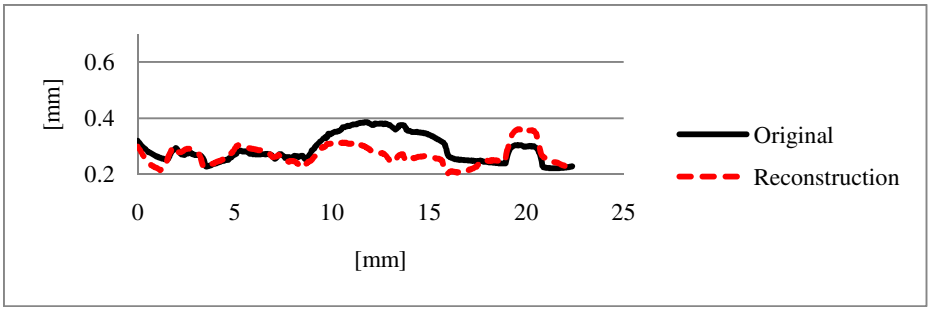

Fig. 9. Comparison of reconstruction of a '20 Kč' coin

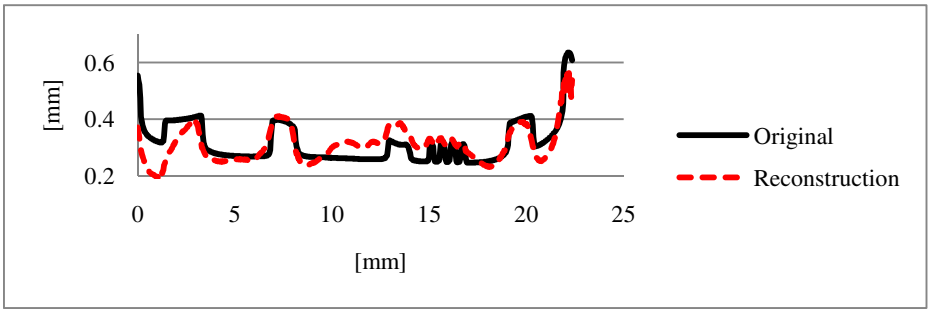

Fig. 10. Comparison of reconstruction of a '5 Kč' coin

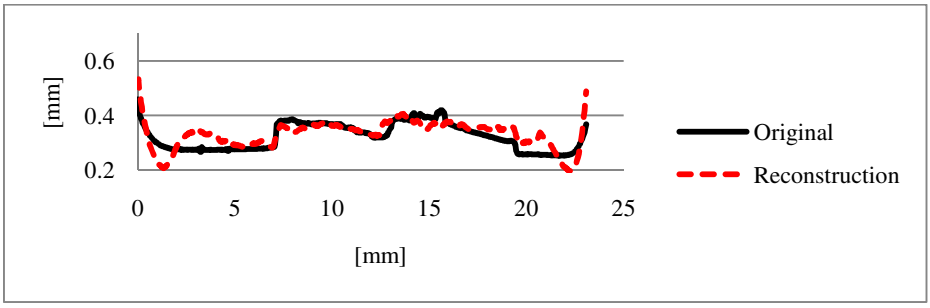

Fig. 11. Comparison of reconstruction of a '10 Kč' coin

9 Future Work

As experiments proved there is a simple method for making duplicates of nearly flat objects on a 3D printer. However, for a practical commercial or non-commercial use several issues have to be solved, especially:

Due to high resolution of a scanner over 4800 dpi large images have to be processed. An object of a size $4 \times 4\ inches$ means solving a system of nearly $369\ mil.$ equations. Resolution used is a critical factor and should be set accordingly to the scanned object. Computed normal map should be preprocessed using some filters to avoid unnecessary distortion and possibly get more precise results.

Texture mapping from the scanned images to the model with a final 3D print with a texture would give the user an opportunity to utilize the already acquired material information.

Representing and respecting material properties of a scanned object, which influences the normal map computation, e.g. surface roughness, could give better results.

10 Conclusion

A novel approach for 3D surface reconstruction and making 3D nearly flat objects replicas using 3D printer is presented. Experiments made proved expected basic properties of the proposed approach. Experiments also proved high precision of reconstruction even when a cheap commodity flatbed scanner is used.

Several types of objects were successfully reconstructed, including glossy coins or fine fabrics.

The presented approach is applicable to $2\,^1/_2$ dimensional, nearly flat objects only and therefore cannot be extended to higher dimensions.

Presented algorithms were implemented on .NET platform for 32 and 64 bits.

Future work will be concentrated on application of Radial Basis Function approximation and optimization of computation.

Acknowledgments. The authors express their thanks to colleagues at the University of West Bohemia and Shandong University for their help and to anonymous reviewers for their critical comments and advices.

The research was supported by the Ministry of Education of the Czech Republic, projects No.LH12181, ME10060, SGS-2013-029 and by China-Czech Scientific and Technological Collaboration Project (40-8), Shandong Natural Science Foundation of China (Grant No. ZR2010FM046).

References

1. Blinn, J.F.: Simulation of wrinkled surfaces. SIGGRAPH Comput. Graph. 12(3), 286–292 (1978)
2. Chen, T., Goesele, H.P.: Seidel: Mesostructure from Specularity. In: 2006 IEEE Computer Society Conference on Computer Vision and Pattern Recognition (CVPR 2006), vol. 2, pp. 1825–1832. IEEE (2006), doi:10.1109/CVPR.2006.182
3. Clarkson, W., Weyrich, T., Finkelstein, A., Heninger, N., Halderman, J.A., Felten, E.W.: Finger printing Blank Paper Using Commodity Scanners. In: Proceedings of the 2009 30th IEEE Symposium on Security and Privacy (SP 2009), pp. 301–314. IEEE Computer Society, Washington, DC (2009)
4. Johnson, M.K., Adelson, E.H.: Retrographic sensing for the measurement of surface texture and shape. In: 2009 IEEE Conference on Computer Vision and Pattern Recognition, pp. 1070–1077. IEEE (2009), doi:10.1109/CVPRW.2009.5206534
5. Johnson, M.K., Cole, F., Raj, A., Adelson, E.H.: Microgeometry capture using an elastomeric sensor. ACM Trans. Graph. 30(4), Article 46, 8 pages (2011)
6. Liu, X., Hu, M.Y., Zhang, H.P.J., Tong, X., Guo, B., Shum, H.-Y.: Synthesis and rendering of bidirectional texture functions on arbitrary surfaces. IEEE Transactions on Visualization and Computer Graphics 10(3), 278–289 (2004), doi:10.1109/TVCG.2004.1272727
7. Myronenko, A., Song, X.B.: On the closed-form solution of the rotation matrix arising in computer vision problems. CoRR abs/0904.1613 (2009)
8. Pan, R., Skala, V.: Surface Reconstruction with higher-order smoothness. The Visual Computer 28(2), 155–162 (2012) ISSN 0178-2789

9. Pintus, R., Malzbender, T., Wang, O., Bergman, R., Nachlieli, H., Ruckenstein, G.: Photo Repair and 3D Structure from Flatbed Scanners Using 4- and 2-Source Photometric Stereo. In: Ranchordas, A., Pereira, J.M., Araújo, H.J., Tavares, J.M.R.S. (eds.) VISIGRAPP 2009. CCIS, vol. 68, pp. 326–342. Springer, Heidelberg (2010)
10. Skala, V.: Projective Geometry and Duality for Graphics, Games and Visualization - Course SIGGRAPH Asia 2012, Singapore (2012) ISBN 978-1-4503-1757-3
11. Toler-Franklin, C., Finkelstein, A., Rusinkiewicz, S.: Illustration of complex real-world objects using images with normals. In: Proceedings of the 5th International Symposium on Non-Photorealistic Animation and Rendering (NPAR 2007), pp. 111–119. ACM, New York (2007)
12. Woodham, R.J.: Photometric stereo: A reflectance map technique for determining surface orientation from image intensity. In: Proc. 22nd SPIE Annual Technical Symposium, vol. 155, pp. 136–143 (1978)
13. Woodham, R.J.: Photometric Method for Determining Surface Orientation from Multiple Images. Optical Engineering 19(1), 139–144 (1980)